Flexible Temperature and Flow Sensor from Laser-Induced Graphene

Marco Marengo, Giovanni Marinaro and Jürgen Kosel, Senior Member, IEEE

***Abstract*— Herein we present a flexible temperature sensor and a flow speed sensor based on laser-induced graphene. The main benefits arise from peculiar electrical, thermal and mechanical performances of the material thus obtained, along with a cheap and simple fabrication process. The temperature sensor is a negative temperature coefficient thermistor with non-linear response typical of semi-metals. The thermistor shows a 4% decrease of the resistance in a temperature range of 20-60 °C. The flow sensor exploits the piezoresistive properties of laser-induced graphene and can be used both in gaseous and liquid media thanks to a protective polydimethylsiloxane coating. Main characteristics are ultra-fast response and versatility in design offered by the laser technology.**

***Keywords*— Flexible sensors, piezoresistor, thermistor, flow meter, temperature sensor, graphene, polyimide.**

I. Introduction

Since graphene has been firstly fabricated by Novoselov et al. in 2004 [1], a lot of effort has been put into finding possible ways to produce graphene and exploit its outstanding electrical, mechanical and chemical properties [2]. Meanwhile, flexible sensors have seen an increase in interest for applications in wearable devices [3-8]. These two lines of research meet in the fabrication of porous graphene on polyimide (PI) films through laser irradiation. The material thus obtained, defined as laser-induced graphene (LIG), is constituted by conductive patterns on insulating and flexible substrates. These electrodes can be used in different applications in the micro and macro scale, e.g. for artificial throat [9], blood analysis [10], and energy storage [11] to name a few. Herein we investigate the resistance variation when the system undergoes thermal and mechanical external stimuli.

In the first case we want to employ LIG on Kapton as a flexible temperature sensor, that is particularly suited for applications such as health monitoring and electronic skin [12]. The detection of temperature change through resistance variation is typical of thermistors. These devices are divided in two main categories: NTC (Negative Temperature Coefficient) and PTC (Positive Temperature Coefficient). NTC thermistors are made of semiconducting materials (metal oxides) and are characterized by a decrease of the resistance, when the temperature increases, since more electrons are available in the conduction band. PTC thermistors are made of ceramic or plastic materials and exhibit an increase of resistance when the temperature increases. Although many commercially available thermistors possess excellent durability and high sensitivity, they are not biocompatible and only few flexible sensors are currently available on the market.

Concerning the flow sensor, the working principle is based on the deflection of a paddle made of PI, which is detected through a LIG conductive pattern on its top surface. Different flow rates induce different deformations that allow to measure the speed of the flow. This paddle concept with bending induced strain has previously been exploited using magnetic materials and showed promising results [13][14]. Commercially available flow sensors use different working principles such as mechanical movement of a piston, differential pressure (Venturi meter), and thermal gradient. Piezoresistivity, the property of some materials to change their resistance when mechanically deformed, is not commonly used in macroscale flow meters, but it is widely applied in Micro Electro-Mechanical Systems (MEMS) [15]. Usually, in a microscale device the flow is measured through a piezoresistive material deposited on top of a cantilever which bends under fluid pressure. In our flow sensor the LIG acts as the piezoresistive material whereas the PI flexible substrate plays the role of the cantilever. The versatility of design, in combination with the cost-effective fabrication process, allows to obtain sensors that can be used both in micro and macro scale measurements in a wide range of flow speeds.

II. Fabrication and Characterization

A. Flow Sensor

A single-step fabrication process is employed, which allows obtaining the conductive electrodes used as piezoresistors (Fig 1A) on the flexible substrate. A commercial PI film (125 µm thick from DuPont) is used as substrate material. The PI is carbonized through direct CO_2 laser writing (wavelength 10.6 µm, power 2 W, speed 16 mm/s, working distance 3 mm, 1000 pulses per inch). This thermal process has been thoroughly characterized by Lin et al. [16] and we obtained the same structure as shown by SEM and Raman spectroscopy (Fig. 2).

Research reported in this publication was supported by the King Abdullah University of Science and Technology (KAUST). M. Marengo, G. Marinaro and J. Kosel are with the Computer, Electrical and Mathematical Sciences and Engineering Division (CEMSE), King Abdullah University of Science and Technology (KAUST), Thuwal 23955-6900, Saudi Arabia (e-mail: marco.marengo@kaust.edu.sa; giovanni.marinaro@kaust.edu.sa; jurgen.kosel@kaust.edu.sa).

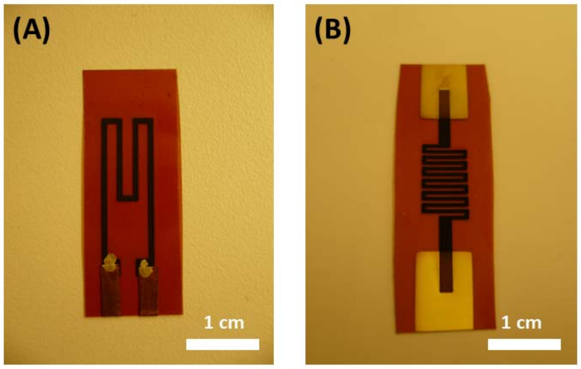

Fig. 1. (A) Flow sensor and (B) temperature sensor. Black lines are the conductive patterns made by laser irradiation on PI film (orange).

The sample is then prepared with the following procedure. First, adhesive copper tape is applied on the two contact pads partially covering them; subsequently, silver paint (purchased from TED Pella, USA) is applied to connect LIG and copper, thus improving the stability of the contacts. Since the experiments are conducted with tap water, a coating is necessary to protect the LIG electrodes from the interaction with ions, which interferes with the measurement due to shunt currents (this step can be avoided if the sensor is used in nonconductive media like air). Few droplets of polydimethylsiloxane (PDMS) with ratio 10(base):1(curing agent) are poured on the center of the device and the sample is placed under vacuum for 20 min to remove air bubbles. Then the PDMS is spread on the surface through spin coating (2000 revolutions per minute for 80 seconds), obtaining a passivation layer that is cured in the oven at 80°C for one hour. The thickness of the PDMS is 20 µm (measured through profilometer).

For testing, the device is inserted into a chamber where flow is applied via a circulation pump. The measurements are performed at room temperature (22°C) and the speed of the water is controlled through the revolutions per minute (rpm) of the pump.

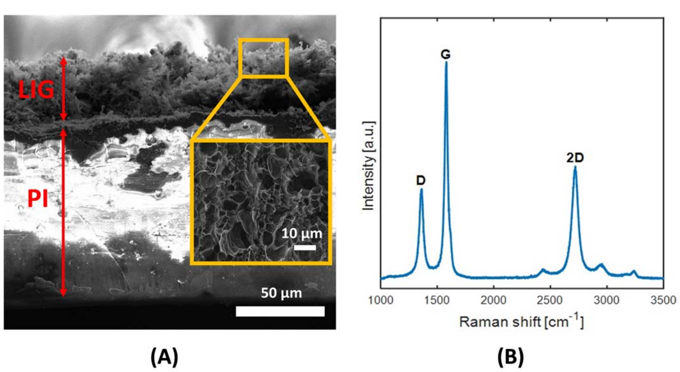

Fig. 2. (A) SEM image of laser induced grapheme (LIG). The cross section of a sample shows the structure of LIG (30 µm thick) on the PI substrate (125 µm thick). The inset shows a zoom-in of the porous structure of the LIG. (B) Raman spectrum of LIG (laser wavelength 473 nm) shows a prominent G peak related to the vibration of sp^2 carbon atoms. The D peak is activated by defects and the 2D peak is the main one in monolayer graphene [17].

B. Temperature Sensor

The fabrication process of LIG on PI is the same as for the flow sensor, but PDMS coating is not used since measurements are performed in air. Moreover, the contacts are made by sputtering 100 nm of gold. The main reason for this is to maintain good electrical contact at elevated temperatures, whereas the glue of the copper tape could melt and ruin the structure of carbon compromising its conductivity (Fig 1B).

III. Results

A. Flow Sensor

First, the chamber used to test the flow sensor is filled with tap water to evaluate the insulation of the PDMS passivation layer. The resistance is measured over a day and no variation is registered. Next, the response to different water flow rates is investigated. A two-wire measurement is carried out through a KEITHLEY 2400 Source Meter with a test current of 1 mA. Due to the turbulence of the water flow the sensor vibrates around the mean value. This phenomenon leads to the noise visible in Fig. 3A, wherein the response of the device to five different flow speeds is shown.

Initially, the speed of the water is zero. Then, it is increased in four steps, which is reflected in increasing sensor resistance. Once the maximum speed is reached, the sensor is exposed again to the first flow speed. The signal returns to the value assumed before, indicating that there is no hysteresis in the sensor response. This test successfully proved the stability of the piezoresistor in fluid media, which is ensured by the PDMS coating. The data points are fit with the moving average fit, allowing to clearly see the step-like response. The flow velocity in this experiment is in the range of 1 m/s. However, the sensor concept provides many degrees of freedom, for the design to accommodate a large dynamic range or sensitivity, since it can be fabricated in different shapes, due to the small laser spot of approximately 100 µm.

B. Temperature Sensor

The response of LIG to a thermal stimulus is investigated through a Cascade Microtech summit 12000 AP probe station equipped with an ETC 200L Thermal Chuck for sample heating. The sensor is placed on the sample holder and surrounded by a metallic chamber to improve the insulation from the environment. A first measurement is acquired at room temperature. Subsequently, the thermal chuck is used to raise the temperature. Before acquiring the next measurement, the sample is left at constant temperature for one hour to ensure that the system has reached thermal equilibrium. The result is shown in Fig. 3B.

The response shows a resistance decrease with temperature, which is typical of NTC thermistors, confirming that the porous structure is mainly constituted by few layers of carbon atoms that behave like semi-metals. It is worth to mention that the response is also influenced by the different coefficient of thermal expansion of LIG and PI, making the theoretical analysis not straightforward.

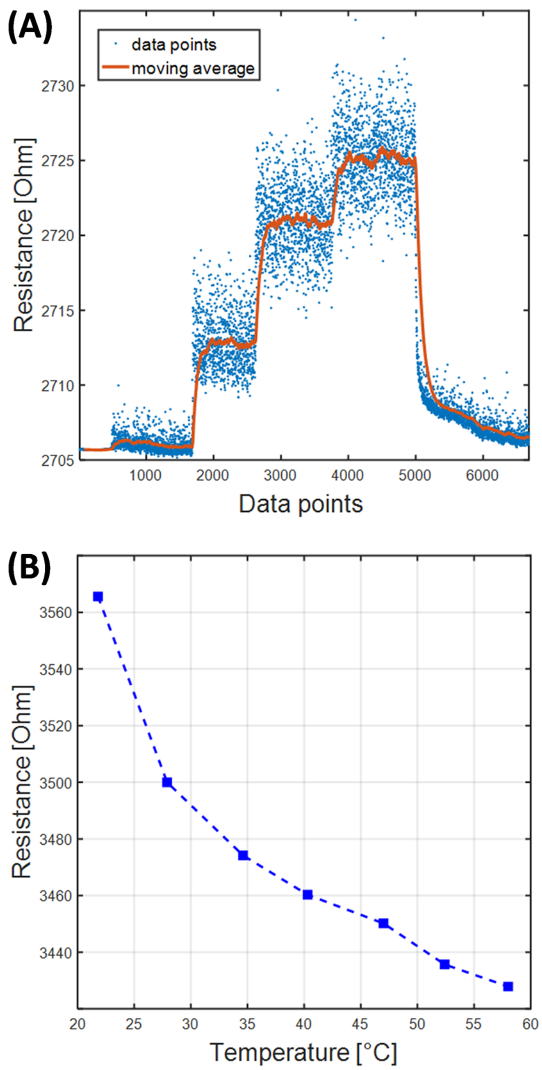

Fig. 3. (A) Response of the flow sensor to five different flow velocities (0, 1500, 2500, 3500, 4500 rpm). 70 data points are used to compute each data point of the moving average. The sampling rate is 7 data points per second. (B) The resistance of the laser induced graphene temperature sensor as a function of temperature.

IV. Conclusion

A flexible temperature sensor and a flow sensor are fabricated by the same method and on the same substrate, i.e. by laser-induced graphene electrodes on Kapton. The polyimide film serves as flexible insulating substrate while the porous carbon structure induced by laser irradiation is the sensing material. The flow sensor is based on piezoresistive properties of porous graphene and it is coated with a thin layer of PDMS to provide a wider spectrum of applications both in fluid and gaseous media. Furthermore, the fast response and the simple fabrication process make this sensor suitable for a wide range of applications. The temperature sensor shows approximately 4% decrease in resistance when the temperature is raised from 22°C to 58°C.

The results show the high versatility of the materials and fabrication process used. Size and shape can be easily optimized for different applications in micro and macro scale. Both sensors are flexible, light weight and cheap, making this concept attractive for wearable and multifunctional sensors.

References

[1] Novoselov, K. S., Geim, A. K., Morozov, S. V, Jiang, D., Zhang, Y., Dubonos, S. V, Firsov, A. A. *et al.* (2004). Electric Field Effect in Atomically Thin Carbon Films. *Science*, *306*(5696), 666 LP-669.on Electricity and Magnetism, 3rd ed., vol. 2. Oxford: Clarendon, 1892, pp.68–73.

[2] Novoselov, K. S., Fal, V. I., Colombo, L., Gellert, P. R., Schwab, M. G., Kim, K., Kim, K. *et al.* (2013). A roadmap for graphene. *Nature*, *490*(7419), 192–200.

[3] Pang, C., Lee, C., and Suh, K. Y. “Recent advances in flexible sensors for wearable and implantable devices.” (2013) *Journal of Applied Polymer Science*, *130*(3), 1429–1441.

[4] A. Alfadhel, J. Kosel, “Magnetic Nanocomposite Cilia Tactile Sensor,” *Advanced Materials*, 27, 47, pp. 7888-7892 (2015).

[5] A. Alfadhel, M.A. Khan, S.C. Freitas, J. Kosel, “Magnetic Tactile Sensor for Braille Reading,” IEEE Sensors Journal 16, 24, pp 8700-8705 (2016).

[6] A. Nag, S.C. Mukhopadhyay, J. Kosel, “Flexible carbon nanotube nanocomposite sensor for multiple physiological parameter monitoring,” Sensors and Actuators A: Physical, 251, pp. 148–155 (2016).

[7] Rojas, J. P., Conchouso, D., Arevalo, A., Singh, D., Foulds, I. G., & Hussain, M. M. (2017). Paper-based origami flexible and foldable thermoelectric nanogenerator. *Nano Energy*, *31*, 296-301.

[8] Nassar, J. M., Mishra, K., Lau, K., Aguirre□Pablo, A. A., & Hussain, M. M. (2017). Recyclable Nonfunctionalized Paper□Based Ultralow□Cost Wearable Health Monitoring System. *Advanced Materials Technologies*, *2*(4).

[9] Tao, L.-Q., Tian, H., Liu, Y., Ju, Z.-Y., Pang, Y., Chen, Y.-Q., Ren, T.-L. *et al.* (2017). An intelligent artificial throat with sound-sensing ability based on laser induced graphene. *Nature Communications*, *8*, 14579.

[10] Fenzl, C., Nayak, P., Hirsch, T., Wolfbeis, O. S., Alshareef, H. N., Baeumner, A. J. (2017). Laser-Scribed Graphene Electrodes for Aptamer-Based Biosensing. *ACS Sensors*.

[11] Peng, Z., Ye, R., Mann, J. A., Zakhidov, D., Li, Y., Smalley, P. R., Lin, J., Tour, J. M. (2015). Flexible Boron-Doped Laser Induced Graphene Microsupercapacitors. *ACS Nano*, (Cc), 1–17.

[12] Li, Q., Zhang, L. N., Tao, X. M., and Ding, X. (2017). Review of Flexible Temperature Sensing Networks for Wearable Physiological Monitoring. *Advanced Healthcare Materials*.

[13] S. Traxler, J. Kosel, H. Pfützner, E. Kaniusas, L. Mehnen, and I. Giouroudi, “Contactless flow detection with magnetostrictive bilayers,” *Sensors Actuators A Phys.*, vol. 142, no. 2, pp. 491–495, 2008.

[14] L. Mehnen *et al.*, “Magnetostrictive bilayer sensors—a survey,” *J. Alloys Compd.*, vol. 369, no. 1, pp. 202–204, 2004.

[15] Nguyen, N. T. (1997). Micromachined flow sensors—a review. *Flow Measurement and Instrumentation*, *8*(1), 7–16.

[16] Lin, J., Peng, Z., Liu, Y., Ruiz-Zepeda, F., Ye, R., Samuel, E. L. G., Yakobson, B. I., Tour, J. M. (2014) Laser-induced porous graphene films from commercial polymers. *Nature Communications*, *5*(5714), 1–8.

[17] Ferrari, A. C., Meyer, J. C., Scardaci, V., Casiraghi, C., Lazzeri, M., Mauri, F., Geim, A. K. *et al.* (2006). Raman spectrum of graphene and graphene layers. *Physical review letters*, *97*(18), 187401.